

# Lawrence Berkeley National Laboratory

## Recent Work

### Title

ABSORPTION, PHOTOLUMINESCENCE AND RESONANT RAMAN SCATTERING IN BI13

### Permalink

<https://escholarship.org/uc/item/4b77069h>

### Authors

Petroff, Yves

Yu, Peter Y.

Shen, Y.R.

### Publication Date

1973-08-01

ABSORPTION, PHOTOLUMINESCENCE AND  
RESONANT RAMAN SCATTERING IN  $\text{BiI}_3$

Yves Petroff, Peter Y. Yu, and Y. R. Shen

RECEIVED  
LAWRENCE  
RADIATION LABORATORY

August 1973

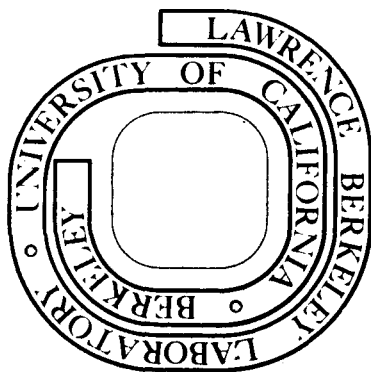
JAN 29 1974

LIBRARY AND  
DOCUMENTS SECTION

Prepared for the U. S. Atomic Energy Commission  
under Contract W-7405-ENG-48

**For Reference**

Not to be taken from this room



## **DISCLAIMER**

This document was prepared as an account of work sponsored by the United States Government. While this document is believed to contain correct information, neither the United States Government nor any agency thereof, nor the Regents of the University of California, nor any of their employees, makes any warranty, express or implied, or assumes any legal responsibility for the accuracy, completeness, or usefulness of any information, apparatus, product, or process disclosed, or represents that its use would not infringe privately owned rights. Reference herein to any specific commercial product, process, or service by its trade name, trademark, manufacturer, or otherwise, does not necessarily constitute or imply its endorsement, recommendation, or favoring by the United States Government or any agency thereof, or the Regents of the University of California. The views and opinions of authors expressed herein do not necessarily state or reflect those of the United States Government or any agency thereof or the Regents of the University of California.

0 5 8 8 3 9 0 7 7 4 7

Submitted to Physica Status Solidi

LBL-1890

UNIVERSITY OF CALIFORNIA

Lawrence Berkeley Laboratory  
Berkeley, California

AEC Contract No. W-7405-eng-48

ABSORPTION, PHOTOLUMINESCENCE AND RESONANT RAMAN  
SCATTERING IN  $\text{BiI}_3$

Yves Petroff<sup>†</sup>, Peter Y. Yu, and Y. R. Shen

August 1973

<sup>†</sup> On leave from University of Paris, France

Absorption, Photoluminescence and Resonant Raman  
Scattering in  $\text{BiI}_3$

Yves Petroff<sup>†</sup>, Peter Y. Yu, and Y. R. Shen

Department of Physics, University of California  
and  
Inorganic Materials Research Division,  
Lawrence Berkeley Laboratory,  
Berkeley, California 94720

ABSTRACT

We have measured the absorption, photoluminescence, and resonant Raman scattering in  $\text{BiI}_3$  at low temperatures with a tunable dye laser. Our results do not support the "bielelectron" model of Gross et al.

Absorption, Photolumineszenz und der resonante Ramaneffekt wurde an  $\text{BiI}_3$  bei tiefen Temperatur mit Hilfe eines durchstimmbaren Farbstofflasers gemessen. Die Ergebnisse können nicht in Rahmen des „Zweielektronenmodells“ (Gross et al.) erklärt werden.

### I. Introduction

Recently Gross and coworkers<sup>1-4</sup> have reported observing a series of lines in the absorption and luminescence spectra of  $\text{BiI}_3$ . The frequencies of these lines seem to obey the equation:

$$\nu_n = \nu_\infty + \frac{R}{n^2} = 15,978 + \frac{1995}{n^2} \text{ cm}^{-1} \quad (1)$$

with  $n = 3, 4, 5, 6$ , and  $7$ . This series converges towards the low frequency side and therefore has the form of an "inverted" hydrogenic series.

Gross et al.<sup>1-4</sup> suggested that this series is due to the formation of "bielectrons" or "biholes" in the crystal. A bielectron (or bihole) is formed by two electrons (or holes) with a negative reduced mass and coupled to each other by Coulomb interaction to form a hydrogen-like bound state with energies given by an inverted hydrogenic series.

The question whether such bielectrons or biholes can exist or not is an interesting one. So far, to our knowledge, there has been no direct experimental evidence on their existence. Although the bielectron model can account for the energy of certain absorption and luminescence lines observed by Gross et al., there are difficulties in reconciling this model with other optical properties of  $\text{BiI}_3$ . We have therefore repeated the experiments of Gross et al. and, in addition, we have measured the luminescence excitation spectrum (LES) and the resonance Raman scattering<sup>5</sup> (RRS) in  $\text{BiI}_3$  using a CW tunable dye laser. We found that our results cannot be explained by the bielectron model. We are led to conclude that the line spectra observed by Gross et al. in  $\text{BiI}_3$  is probably due to impurities or defects as suggested by Timofeev and Vashchenko.<sup>6</sup>

## II. Review on Properties of $\text{BiI}_3$ and the Bielectron Model

$\text{BiI}_3$  crystallizes in layers with trigonal symmetry<sup>7</sup> (space group  $C_{3i}^2$ ).

Reflectivity and absorptivity of  $\text{BiI}_3$  have been measured by a number of authors at liquid nitrogen and room temperatures.<sup>8-11</sup> According to most authors, above the absorption edge of  $\text{BiI}_3$  there are a number of sharp peaks, probably due to formation of excitons. By interpreting these peaks as being formed from a p-like valence band split by spin-orbit coupling, Evans<sup>8</sup> obtained the lowest energy gap of  $\text{BiI}_3$  as 2.33 eV and spin-orbit splitting 0.38 eV at 77°K.

Timofeev and Vashchenko<sup>6</sup> found that at 20.4°K non-stoichiometric  $\text{BiI}_3$  crystals showed absorption lines at 6166, 6205, 6221, 6231, and 6409 Å below the fundamental edge. These lines disappeared at 90°K except the 6409 Å line. Later Gross et al.<sup>1,2</sup> also observed these lines in both absorption and photoluminescence spectra of  $\text{BiI}_3$  at 4.2°K. They noted that the first four lines fitted an "inverted" hydrogenic series (Eq. 1) very well and with increase in temperature these lines shifted towards higher energies while the absorption edge shifted in the opposite direction. These observations and subsequent experiments<sup>3,4</sup> led them to propose the "bielectron" (or bihole) model.

In their bielectron model<sup>2,4</sup> (see Figure 1) a conduction band  $C_1$  is partially filled while a higher conduction band  $C_2$  is empty. In analogy with an exciton<sup>12</sup> the wave function of a system of two electrons (bielectrons), one in  $C_1$  and one in  $C_2$ , is given by

$$\Psi_{n,\bar{k}} = \sum_{\bar{k}_1, \bar{k}_2} \phi_{\bar{k}_1, \bar{k}_2}^{n, \bar{k}} \psi_{\bar{k}_1}(\bar{r}_1) \psi_{\bar{k}_2}(\bar{r}_2) \quad (2)$$

where  $\psi_{\bar{k}_1}(\bar{r}_1)$  and  $\psi_{\bar{k}_2}(\bar{r}_2)$  are the wave functions of the electrons in  $C_1$  and  $C_2$  respectively and  $\phi_{\bar{k}_1, \bar{k}_2}^{n, k}$  is the envelope function. The Fourier transform  $\phi(\bar{r}_1, \bar{r}_2)$  of  $\phi_{\bar{k}_1, \bar{k}_2}^{n, k}$  satisfies the equation:

$$\left\{ E_1(\bar{k}_1) + E_2(\bar{k}_2) + \frac{e^2}{\epsilon |\bar{r}_1 - \bar{r}_2|} \right\} \phi(\bar{r}_1, \bar{r}_2) = (E - E_0) \phi(\bar{r}_1, \bar{r}_2) \quad (3)$$

where  $E_1(\bar{k}_1)$  and  $E_2(\bar{k}_2)$  are the energy operators of an electron in  $C_1$  and  $C_2$  respectively;  $E$  is the energy of the bielectron;  $E_0$  is the energy difference between  $C_1$  and  $C_2$  at  $k=0$ ;  $e$  is the charge of the electron and  $\epsilon$  is the dielectric constant. It is well-known that the effective mass approximation  $\phi(\bar{r}_1, \bar{r}_2)$  can be written as<sup>12</sup>:

$$\phi(\bar{r}_1, \bar{r}_2) = e^{i\bar{k} \cdot \bar{R}} \phi(\bar{r}) \quad (4)$$

where  $\bar{r} = \bar{r}_1 - \bar{r}_2$ ,  $\bar{R} = \frac{m_1 \bar{r}_1 + m_2 \bar{r}_2}{m_1 + m_2}$  (assuming  $C_1$  and  $C_2$  are spherical bands with effective masses  $m_1$  and  $m_2$  respectively) and  $\phi(\bar{r})$  satisfies the equation:

$$\left( \frac{p^2}{2\mu} + \frac{e^2}{\epsilon r} \right) \phi(\bar{r}) = (E - E_0) \phi(\bar{r}). \quad (5)$$

In Eq. (5)  $\mu$  is the reduced mass of the bielectron and is given by

$$\frac{1}{\mu} = \frac{1}{m_1} + \frac{1}{m_2}. \quad (6)$$

If  $\mu$  is positive, the electrons repel each other and no bound state is formed. However, if the curvatures of  $C_1$  and  $C_2$  are such that  $\mu$  is negative then it is possible for Eq. (5) to have bound state solutions with energies given by:

$$E = E_0 + \frac{\mu e^4}{2\hbar^2 \epsilon^2 n^2} \quad n = 1, 2, 3, \dots \quad (7)$$

According to Eq. (7) the absorption spectrum of a bielectron will consist of an "inverted" hydrogenic series. By choosing the right symmetries



for  $C_1$  and  $C_2$ , Gross et al.<sup>2</sup> showed that it is possible to explain why the  $n=1$  and 2 lines are not observed.

### III. Experimental Details

The single crystals of  $\text{BiI}_3$  used in our experiments were grown from 99.999% pure  $\text{BiI}_3$  powder<sup>13</sup> using the method of Evans.<sup>8</sup> They were in the form of platelets with the c-axis perpendicular to the plane surfaces. A typical platelet measures  $25 \text{ mm}^2$  in area and about  $100 \mu$  in thickness. Measurements have been performed mainly on three samples (referred to as samples A, B, and C) from three different melts. The difference between these samples is that sample A was the result of our first attempt to grow these crystals, while samples B and C were grown more carefully from  $\text{BiI}_3$  crystals which had been recrystallized. In particular, sample C was grown very carefully in a length of two days from crystals which had been recrystallized three times.

All optical measurements were conducted on the as-grown surfaces without further treatment. Care was taken not to expose the crystals to air for more than a few minutes since the crystals are attacked by air gradually. All measurements were performed with the crystals immersed in liquid or gaseous He. The luminescence and Raman spectrum were excited by a tunable CW dye laser (Spectra Model 70) with typical output powers of  $\sim 50 \text{ mW}$  and linewidth  $\sim 0.5 \text{ \AA}$ . The use of a tunable laser enabled us to measure the luminescence excitation spectrum and the dispersion of the resonant Raman scattering.

#### IV. Absorption, Luminescence and Resonant Raman Scattering in $\text{BiI}_3$

##### A. Absorption

Figure 2 shows the absorption spectrum of  $\text{BiI}_3$  (sample A) near the absorption edge obtained at 1.8°K. It is very similar to that reported by Gross et al.<sup>1,2</sup> For ease of reference we have labeled the peaks as A, B, C and so on. The peaks A, C, D and E have been found by Gross et al. to coincide in energy with the  $n = 3, 4, 5$  and 6 members of an inverted hydrogenic series (Eq. 1). We note that the structures F and G do not fit the series. They have also been observed by Gross et al. but no explanation was offered for their origin. In particular the G line has been studied in detail by Timofeev and Vashchenko<sup>6</sup> who suggested that it is associated with impurity centers in the crystal.

When the temperature was increased we found all the lines (including F and G) broadened, weakened, and shifted towards higher energies. This is contrasted by the shift towards lower energies of the absorption edge and other optical structures at higher energies.<sup>14</sup> We also found that the intensity of all these structures, except the peak A, depends strongly on the sample. These structures were strongest in sample A, much weaker in sample B, and almost undetectable in sample C.

##### B. Luminescence

The luminescence spectrum of  $\text{BiI}_3$  (sample A) at 4.2°K excited by a CW dye laser is also shown in Figure 2 for comparison with the absorption spectrum. Unlike the absorption spectrum, our luminescence spectrum is somewhat different from that reported by Gross et al.<sup>2</sup> Their spectrum shows a huge broad band below  $16,100 \text{ cm}^{-1}$  with sharp peaks superimposed on it. This is absent in our spectrum. We believe this broad background

is probably due to impurities or defects in the crystal.

In general, the luminescence spectra of all three samples we have studied are similar. However, there is a slight difference between samples A and C below  $16,100 \text{ cm}^{-1}$ . The luminescence of sample C in this region is shown in the insert of Figure 2. It shows the appearance of the peak D and the absence of the fine structures in F.

The luminescence excitation spectrum of the line C is shown in Figure 2. We note that the luminescence appears only when the incident photon energy is above the fundamental absorption edge ( $E_g$ ) at  $16,210 \text{ cm}^{-1}$ . Also, the entire luminescence spectrum appeared or disappeared en bloc. No luminescence was detected when the exciting frequency fell on one of the absorption lines. Attempts to study the polarization dependence of the luminescence spectrum were not successful because of the difficulty in preparing a sample surface parallel to the c-axis.

### C. Resonant Raman Scattering

So far there have been very few theoretical or experimental studies<sup>15</sup> on the phonon spectrum of  $\text{BiI}_3$ . There are six atoms in each unit cell of  $\text{BiI}_3$  so there are twenty-one zone-center optical phonons. Of these twelve are infrared active and the rest are Raman active. To our knowledge no infrared measurements on crystalline  $\text{BiI}_3$  have been reported<sup>15</sup> and only Raman studies of powdered crystals of  $\text{BiI}_3$  have been performed by Kiefer.<sup>16</sup> He observed Raman lines corresponding to phonon energies  $116, 140, \text{ and } 176 \text{ cm}^{-1}$ .

Due to the shape of our samples, all Raman spectra were obtained in the back-scattering geometry on the surface perpendicular to the c-axis. In this geometry, we have only two possible polarization

configurations: (a) polarization of the incident light ( $\hat{e}_i$ ) parallel to that of the scattered light ( $\hat{e}_s$ ) and (b)  $\hat{e}_i \perp \hat{e}_s$ . From the symmetry of the Raman tensor<sup>17</sup> for  $C_{3i}^2$  we found that all three Raman-active modes ( $\Gamma_1$ ,  $\Gamma_2$  and  $\Gamma_3$ ) are allowed for case (a) while only  $\Gamma_2$  and  $\Gamma_3$  modes are allowed for case (b). Thus, with our scattering geometry we can deduce only the symmetry of the  $\Gamma_1$  modes. Also the frequencies of our laser output are in the region of resonance so that the selection rules can be complicated by resonance effects.<sup>18</sup>

Figure 3(a) shows a Raman spectrum of  $\text{BiI}_3$  excited by the dye laser with frequency  $16,011 \text{ cm}^{-1}$  which is below the absorption edge. This particular spectrum was obtained with sample C but unlike the luminescence and absorption spectra there was no difference between the Raman spectra of all three samples. In Figure 3(a) we see one very strong and sharp Raman line at  $111 \pm 2 \text{ cm}^{-1}$  and much weaker lines at 56, 94, and  $220 \text{ cm}^{-1}$ . The symmetry of the 56, 111, and  $220 \text{ cm}^{-1}$  lines was found to be  $\Gamma_1$ .

As the frequency of the dye laser was varied, new Raman lines began to appear and disappear indicating that there were strong resonance effects. As an example, Figure 3(b) shows the Raman spectrum of  $\text{BiI}_3$  excited by a  $16,356 \text{ cm}^{-1}$  laser. The Raman lines, denoted by R, are now superimposed on the luminescence. We note that the weak  $220 \text{ cm}^{-1}$  line in Figure 3(a) is now as strong as the  $110 \text{ cm}^{-1}$  line while a new line appears at  $132 \text{ cm}^{-1}$ . By varying the dye laser frequency between  $16,000 \text{ cm}^{-1}$  and  $17,550 \text{ cm}^{-1}$ , we have observed a total of 11 lines in the Raman spectrum of  $\text{BiI}_3$ : 40, 56, 76, 94, 111, 132, 149, 165, 186, 220, and  $243 \text{ cm}^{-1}$ . We have also observed breakdown in the selection rule of

some of the lines at resonance.

Figure 4 shows the variation in the intensity of the scattered light (after correction for dispersion in the optical system) as a function of incident photon energies for a few of the stronger Raman lines. Around the absorption edge the absorption coefficient usually changes rapidly and it is often necessary to correct the data for the change in the penetration depth of light by multiplying the cross-section by the sum of the incident and scattered absorption constants.<sup>19</sup> As we do not have reliable data on the absorption coefficients of  $\text{BiI}_3$  above the absorption edge at  $4.2^\circ\text{K}$ , this effect has not been corrected for in Figures 4 and 5. However, we should point out that since the structures in the Raman intensity shown in Figures 4 and 5 are very sharp compared to the smooth absorption curve of samples B and C (in which resonant Raman scattering was measured), this absorption correction should not introduce any new structures nor change the position of the structures in Figures 4 and 5. Therefore, our discussion in the next section will not be affected by this correction. In Figure 4 we have also shown the reflectivity spectrum of  $\text{BiI}_3$  ( $4.2^\circ\text{K}$ ) in this frequency range. The strong maximum at  $16,750 \text{ cm}^{-1}$  has been reported before<sup>8,10</sup> and has been suggested to be excitonic in nature.

Figure 5 shows the dispersion of the intensity of six Raman lines of  $\text{BiI}_3$  in the region of the "bielectron" series. The curves have been displaced vertically for clarity. We note that all six curves show some structures in this frequency region but most of the sharper structures do not coincide in energy with any of the lines A, B, and C, etc. In fact, they tend to occur inside the absorption continuum where

there are no sharp structures in the optical spectrum. Also there appears to be no correlation between the position of the peaks in different Raman lines. This is no longer true if we plot the intensity of these lines as a function of the frequency of the scattered photon. The result is shown in Figure 6. We now find that the sharp structures in Figure 5 all fall on one of lines A, B, C, and so on. Clearly the strong peaks in the intensity of the  $220 \text{ cm}^{-1}$  and  $130 \text{ cm}^{-1}$  lines are due to resonance of their scattered photon frequency with the strong line C in the luminescence.

#### V. Discussion

Before discussing our results on  $\text{BiI}_3$  and their interpretation with respect to the bielectron model of Gross et al., it is important to stress that our experimental results basically agree with those of Gross et al.

In their papers, Gross et al. have based their bielectron model mainly on the fact that some of the lines they observed obey an inverted hydrogenic series. They did not explain why the lines F and G were not included in the series, although our results indicate that they are not different from the other lines. There was also no attempt to fit the intensity of the different lines to theoretical predictions based on their model. Also, it is not obvious that the bielectron model can explain the unusual temperature coefficient of these lines.

When we tried to explain our luminescence and resonant Raman data with the bielectron model, we ran into difficulties. From the luminescence excitation spectrum we found that all the luminescence disappeared together when the incident photon energy is below the absorption edge.

This absorption edge is generally agreed to be due to electronic transitions from the valence to the conduction band.<sup>8-10</sup> Thus, our result indicates that the incident photon excites an electron from the valence band to the conduction band, the electron or hole relaxes into one of the bielectron or bihole states and then decays radiatively. This process is different from what Gross et al. proposed (as shown in Figure 1). In their model the electron is excited from the partially filled conduction band  $C_1$  to a higher conduction band instead of from the valence band. This model can be reconciled with our result only if this transition coincides exactly in energy with the fundamental absorption edge. This would be very unlikely and furthermore it still fails to explain why the lower bielectron lines (e.g., the C line) were not observed even when the upper bielectron states (e.g., the A line) were excited. It is also difficult to explain the resonance Raman scattering results with the bielectron model. If the bielectron lines were indeed members of the same series it is not obvious why the 220 and 130  $\text{cm}^{-1}$  lines resonate strongly with the C line but not with the other lines or why the 56  $\text{cm}^{-1}$  line resonates with only the A and B lines. We therefore conclude that although the bielectron model is conceptually appealing in explaining the energy of the A, C, D, and E lines, it fails to explain our luminescence and resonant Raman scattering results.

Putting aside the bielectron model, we can nevertheless assert that the lines A, B, C, D, E, F, and G are electronic levels, probably associated with impurity or vacancies in the crystal. They cannot be associated with phonons. If they were, they would appear at low temperatures in either the absorption or the luminescence spectrum, but not both.

This assertion is also supported by our resonant Raman scattering results. If the line C, for example, were a phonon side band of an electronic (or excitonic) level, it is difficult to explain why two apparently unrelated phonons ( $130$  and  $220 \text{ cm}^{-1}$ ) will show resonance at C. On the other hand, if these levels were electronic (or excitonic) it is possible to explain our result. Recently, strong enhancements in Raman cross-section have been observed in  $\text{Cu}_2\text{O}$ <sup>20</sup> when the incident photon energy lies in an absorption continuum and the scattered photon energy is resonant with an excitonic level. In that case, it was shown conclusively that the strong enhancement in the Raman scattering was a consequence of the resonance in both the incident and scattered photon energies (double resonance). It is quite likely that similar double resonances are responsible for the sharp peaks observed in the  $40$ ,  $220$ ,  $130$ , and  $76 \text{ cm}^{-1}$  phonon lines of  $\text{BiI}_3$  (see Figure 6).

Timofeev and Vashchenko<sup>6</sup> found, as we did also, that the sharp lines C, D, and so on in the absorption spectrum depends on the sample and they suggested that these lines are due to excess Bi in the crystal. Our resonance Raman scattering results indicate that the different lines may even be associated with different impurities. It is conceivable that a phonon mode involving mainly, for example, the iodine atoms will couple more strongly to an impurity or vacancy at an iodine site. This can also explain why we can optically excite the A line and do not observe luminescence from the other lines. If interaction between different defect centers are weak, excitation at one center would not be effectively transferred to another center to cause the latter to fluoresce. More studies on samples with controlled impurities will help to



establish the origin of the individual lines. We should point out, however, that no explanation is presently available to account for the temperature dependence of these lines.

In conclusion, we have measured the absorption and luminescence spectra of  $\text{BiI}_3$  at low temperatures. We have confirmed the existence of a series of lines obeying Eq. (1) in those spectra as reported by Gross et al. We have, in addition, measured the luminescence excitation spectra of those lines and the resonances in the Raman scattering around them. We found that our results do not support the bielectron model proposed by Gross et al. Instead, we are led to conclude that these lines are electronic levels associated with impurities or defects in the crystal as has been suggested by Timofeev and Vashchenko.

We are indebted to Prof. C. Kittel for bringing this problem to our attention and for helpful discussions. We are also grateful to Professor M.L. Cohen and L. Falicov for numerous discussions. This work was sponsored under the auspices of the Atomic Energy Commission.

## References

- † On leave from University of Paris, France.
1. E. F. GROSS, V. I. PEREL, and R. I. SKEKHMAMET'EV, ZhETF Pis. Red. 13, 320 (1971); [English Translation: JETP Lett. 13, 229 (1971)].
  2. E. F. GROSS, N. V. STAROSTIN, and R. I. SKEKHMAMET'EV, Fizika Tverdogo Tela 13, 3393 (1971); [English Translation: Soviet Physics--Solid State 13, 2850 (1972)].
  3. E. F. GROSS, I. N. URAL'TSEV, and R. I. SKEKHMAMET'EV, ZhETF Pis. Red. 13, 503 (1971); [English Translation: JETP Lett. 13, 357 (1971)].
  4. E. F. GROSS, N. V. STAROSTIN, M. P. SHEPILOV, and R. I. SHEKHMAMET'EV, Fizika Tverdogo Tela 14, 1942 (1972); [English Translation: Soviet Physics--Solid State 14, 1681 (1973)].
  5. See, for example, T. C. DAMEN and J. SHAH, Phys. Rev. Letters 27, 1506 (1971); and P. Y. YU, Y. R. SHEN, Y. PETROFF, and L. FALICOV, *ibid.* 30, 283 (1973).
  6. V. B. TIMOFEEV and V. I. VASHCHENKO, Opt. Spektr. 24, 740 (1968); [English Translation: Opt. and Spect. 24, 396 (1968)].
  7. J. TROTTER and T. ZOBEL, Z. Krist. 123, 67 (1966).
  8. B. L. EVANS, Proc. Roy. Soc. A289, 275 (1966).
  9. R. I. SHEKHMAMET'EV, Fiz. Tver. Tela 3, 581 (1961); [English Translation: Soviet Phys.--Solid State 3, 426 (1961)].
  10. M. R. TUBBS, J. Phys. Chem. Solids 29, 1191 (1968); Phys. Stat. Solidi 649, 11 (1972).
  11. V. I. VASHCHENKO and V. B. TIMOFEEV, Fiz. Tver. Tela 9, 1577 (1967); [English Translation: Soviet Phys.--Solid State 9, 1242 (1967)];  
V. I. VASHCHENKO, V. B. TIMOFEEV, and I. N. ANTIPOV, Opt. Spekt. 22, 813 (1967); [English Translation: Opt. Spect. 22, 440 (1967)].

12. See, for example, R. S. KNOX, Theory of Excitons (Academic Press, New York, 1963).
13. Atomergic Chemetals Co., Long Island, New York 11514.
14. Y. PETROFF, unpublished.
15. We have observed strong reststrahlen bands in crystalline  $\text{BiI}_3$  at 43, 70, and  $98 \text{ cm}^{-1}$ . We are grateful to K. H. Yang for performing the infrared measurements.
16. W. KIEFER, Z. Naturforsch. 25a, 1101 (1970).
17. R. LOUDON, Advances in Phys. 13, 423 (1964).
18. See, for example, R. M. MARTIN and T. C. DAMEN, Phys. Rev. Letters 26, 86 (1971).
19. R. LOUDON, J. Phys. Radium 26, 677 (1965).
20. P. Y. YU, unpublished.

Figure Captions

Fig. 1. The bielectron model proposed by Gross et al. in Reference 2.

$C_1$  and  $C_2$  are two conduction bands separated by an energy gap  $E_0$ .  $n = 3, 4, 5,$  and  $6$  denote the bielectron levels. Steps 1 and 2 denote the absorption and luminescence processes respectively.

Fig. 2. Absorption, luminescence and luminescence excitation spectra of  $\text{BiI}_3$ . Solid line is the luminescence spectrum of sample A at  $4.2^\circ\text{K}$ . Dotted line is the absorption spectrum of sample A at  $1.8^\circ\text{K}$ . The insert shows the luminescence of sample C in the region where it differs from sample A.  $\text{---} \cdot \text{---} \cdot \text{---}$  is the luminescence excitation spectrum for peak C in sample C at  $4.2^\circ\text{K}$ .

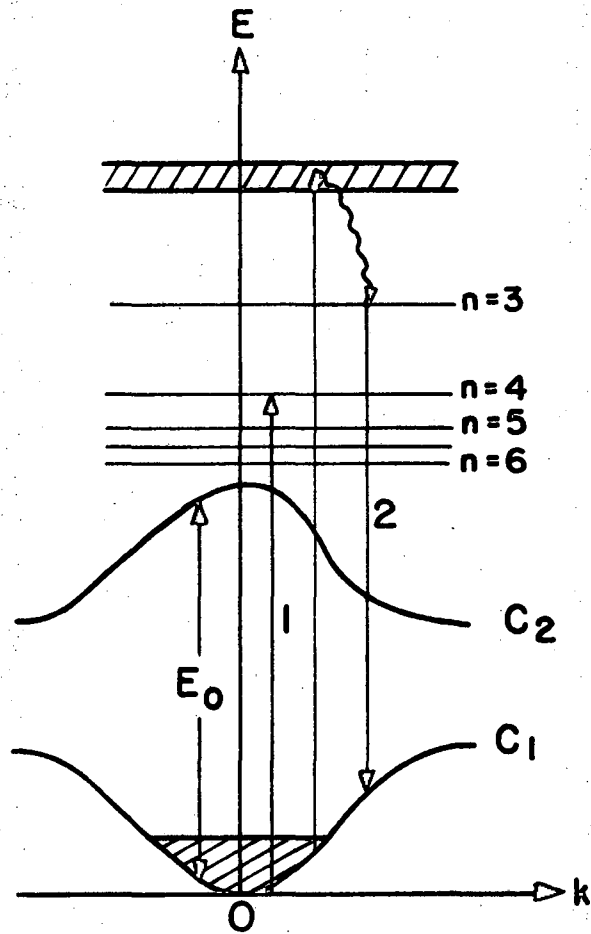
Fig. 3. Raman spectra of  $\text{BiI}_3$  (sample C) at  $4.2^\circ\text{K}$  excited by two different laser frequencies (a)  $16011 \text{ cm}^{-1}$ . (b)  $16356 \text{ cm}^{-1}$ . The peaks denoted by R in (b) are the Raman peaks as distinct from the luminescence peaks A, B, and C.

Fig. 4. Dispersion in the Raman intensity of 4 Raman lines of  $\text{BiI}_3$  (sample C) at  $4.2^\circ\text{K}$ :  $\text{---} \Delta \text{---} \Delta \text{---} 111 \text{ cm}^{-1}$   $\text{---} \circ \text{---} \circ \text{---} 220 \text{ cm}^{-1}$ ,  $\text{---} \cdot \text{---} \cdot \text{---} 56 \text{ cm}^{-1}$ , and  $\text{---} \square \text{---} \square \text{---} \square \text{---} \square \text{---} \square \text{---} \square \text{---} 149 \text{ cm}^{-1}$ . The numbers next to each curve give the factor which the vertical scale has been multiplied for each curve. The solid curve is the reflectivity of  $\text{BiI}_3$  at  $4.2^\circ\text{K}$ .

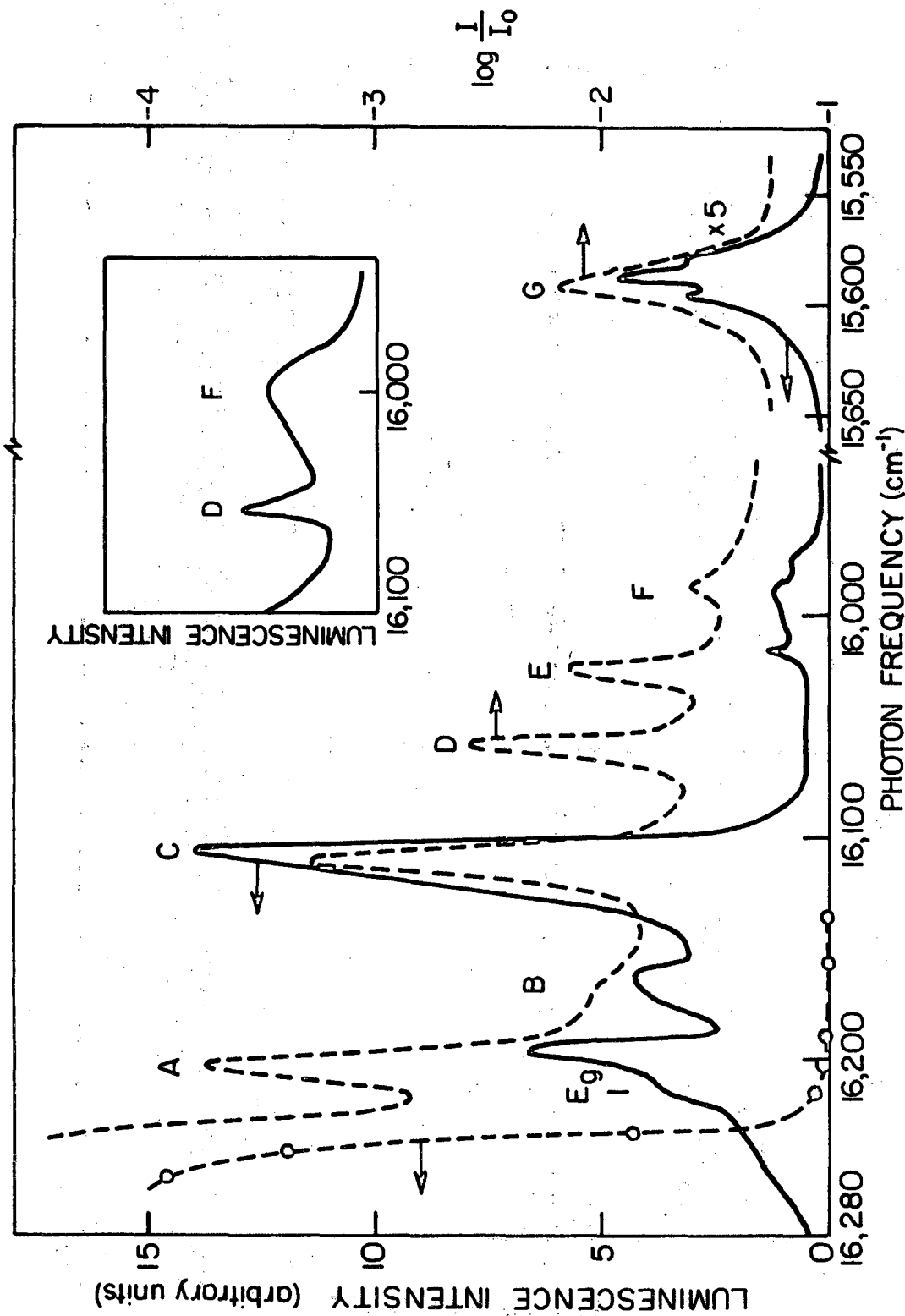
Fig. 5. Dispersion in the Raman intensity of 6 Raman lines of  $\text{BiI}_3$  (sample C) at  $4.2^\circ\text{K}$  as a function of incident photon frequencies:  $\text{---} \Delta \text{---} \Delta \text{---} 111 \text{ cm}^{-1}$ ,  $\text{---} \circ \text{---} \circ \text{---} 220 \text{ cm}^{-1}$ ,  $\text{---} \nabla \text{---} \nabla \text{---} 130 \text{ cm}^{-1}$ ,  $\text{---} \square \text{---} \square \text{---} 40 \text{ cm}^{-1}$ ,  $\text{---} \cdot \text{---} \cdot \text{---} 56 \text{ cm}^{-1}$ , and  $\text{---} \square \text{---} \square \text{---} 76 \text{ cm}^{-1}$ . The zeroes for the vertical axis of the different Raman lines have been displaced vertically for clarity. They are denoted by the

horizontal bars with the corresponding frequency above them. The numbers next to each curve give the factor which the vertical scale must be multiplied for each curve.

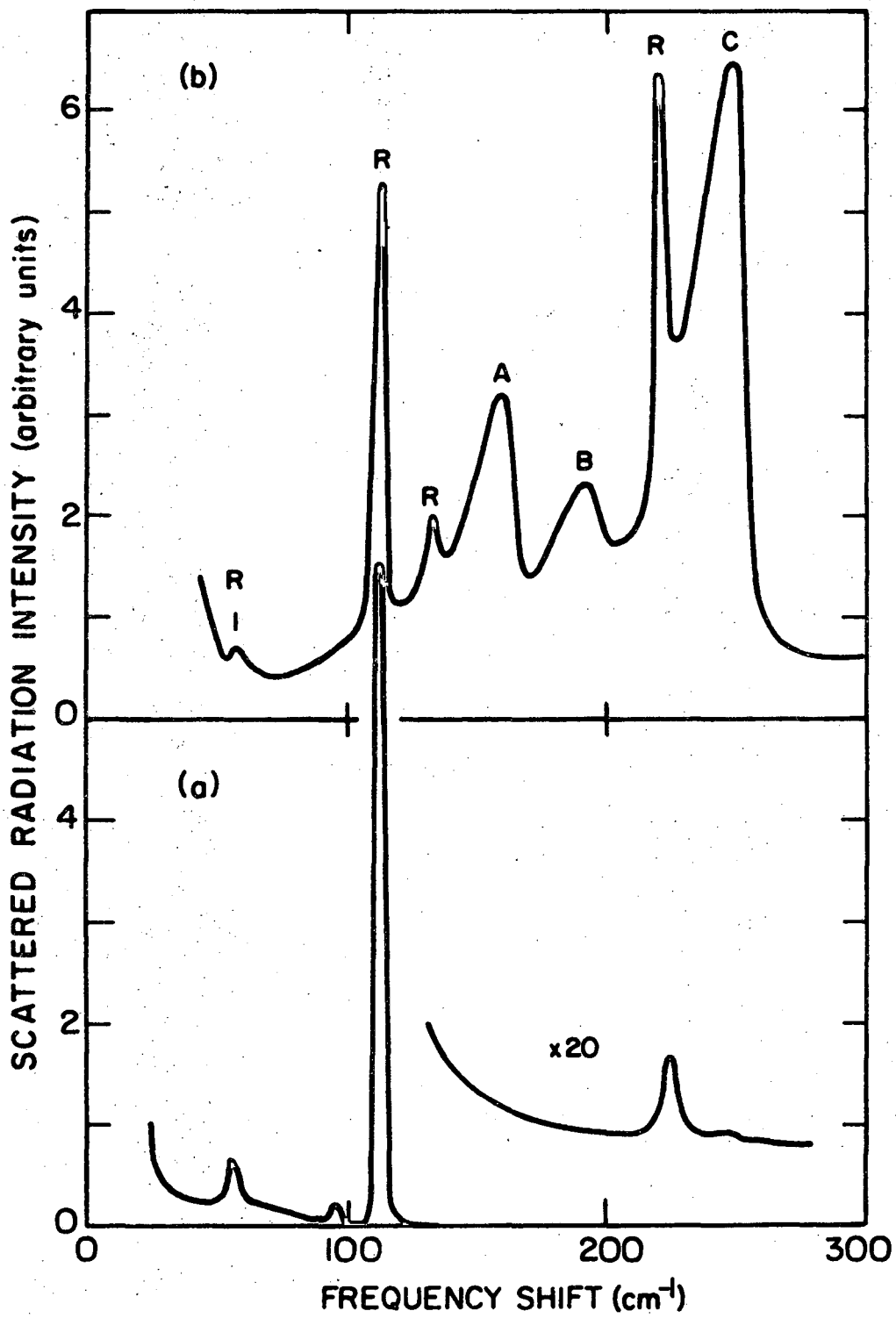
Fig. 6. The curves in Fig. 5 plotted as a function of the frequency of the scattered radiation.



XBL 738-1599

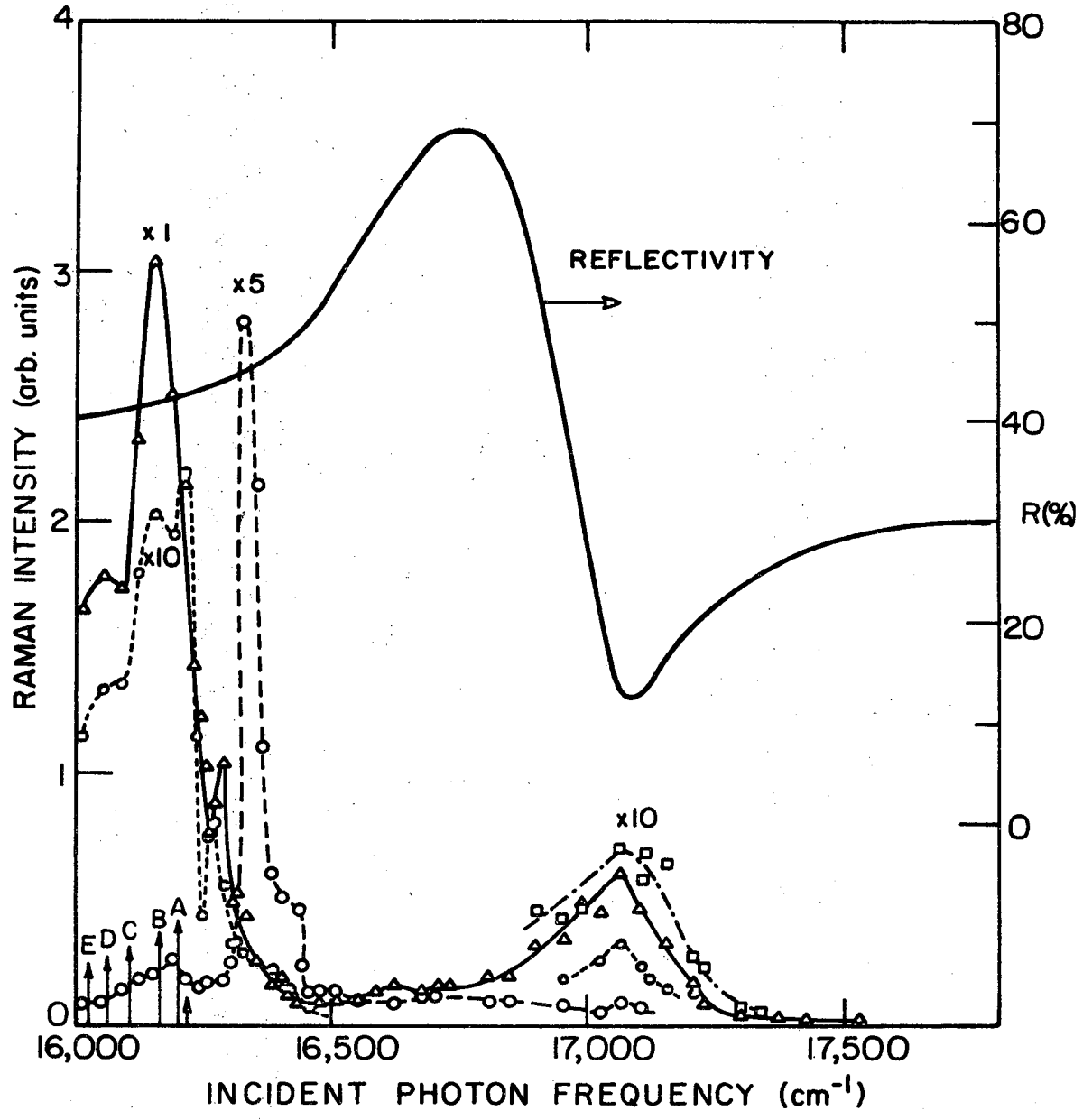


XBL738 - 1600

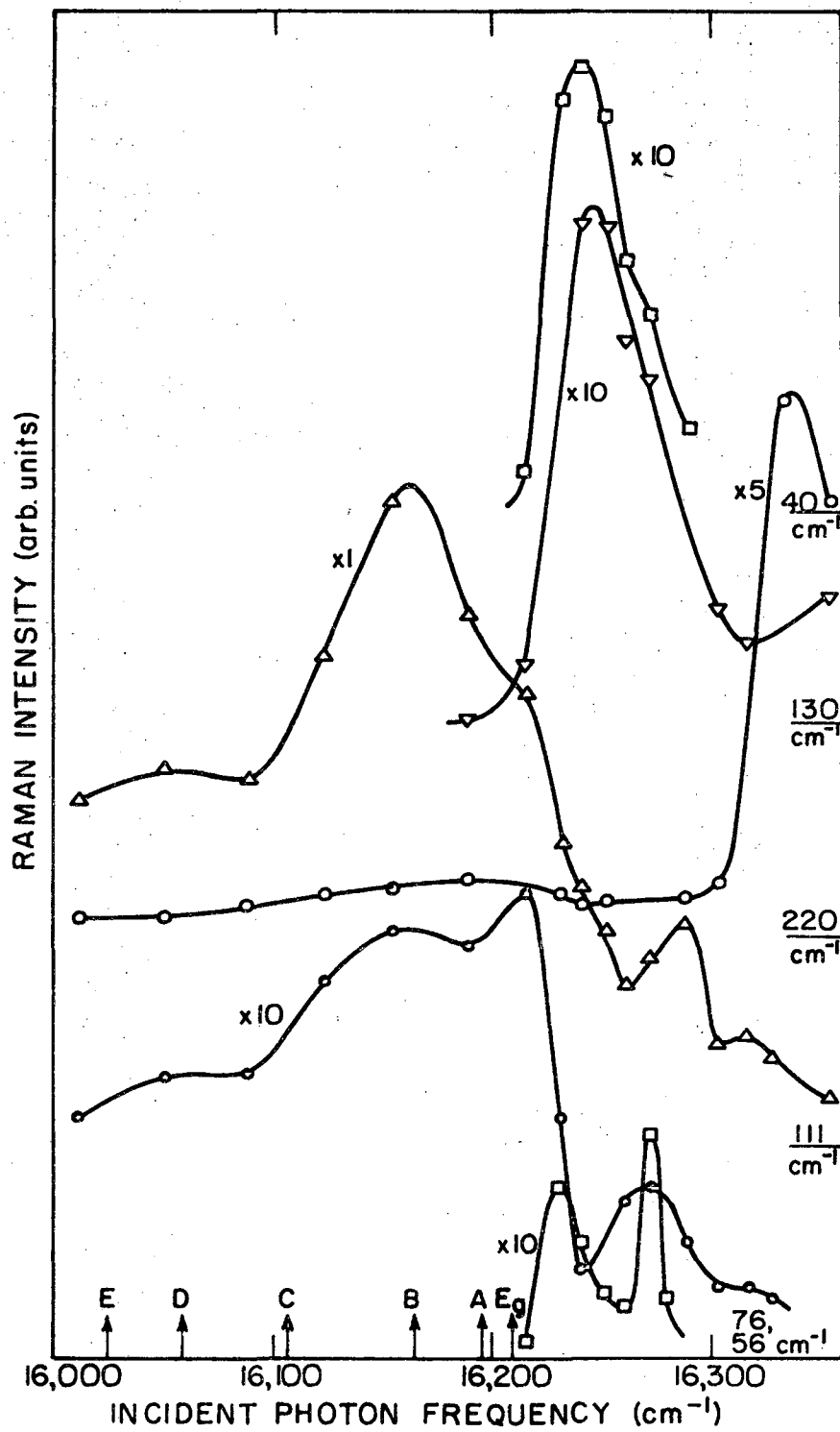


XBL738-1601

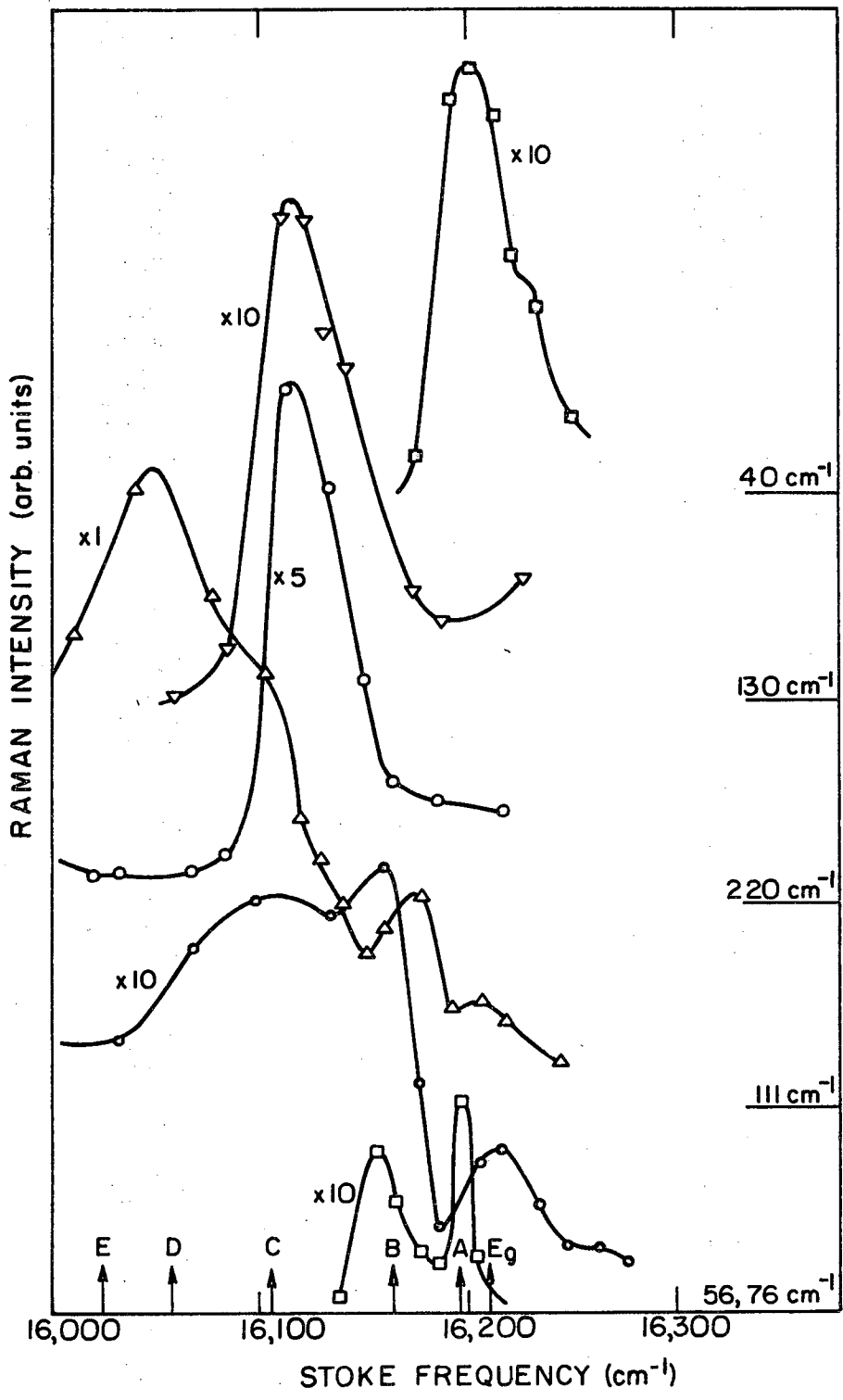




XBL 738-1602



XBL738-1603



XBL738-1604

LEGAL NOTICE

*This report was prepared as an account of work sponsored by the United States Government. Neither the United States nor the United States Atomic Energy Commission, nor any of their employees, nor any of their contractors, subcontractors, or their employees, makes any warranty, express or implied, or assumes any legal liability or responsibility for the accuracy, completeness or usefulness of any information, apparatus, product or process disclosed, or represents that its use would not infringe privately owned rights.*

TECHNICAL INFORMATION DIVISION  
LAWRENCE BERKELEY LABORATORY  
UNIVERSITY OF CALIFORNIA  
BERKELEY, CALIFORNIA 94720